SAND2023-07693C

Sandia National Laboratories

Leveraging Data Driven Frameworks to Build Transferable Interatomic Potentials

Svetoslav Nikolov, John Carpenter, Mitchell Wood, Julien Tranchida, Kyle Cochrane, Normand Modine, Aidan Thompson, Attila Cangi, Kushal Ramakrishna Andrew Rohskopf

ZFS Workshop, 2023

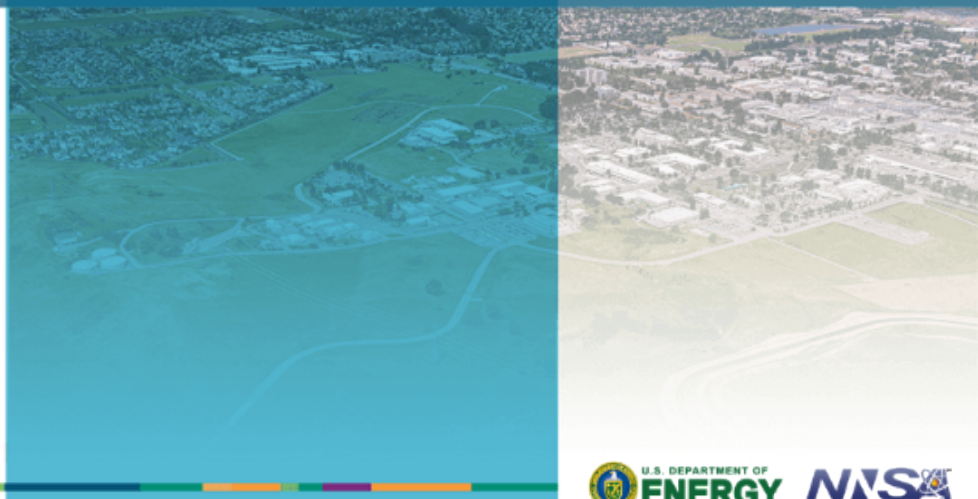

U.S. DEPARTMENT OF ENERGY NNSA

Sandia National Laboratories is a multimission laboratory managed and operated by National Technology & Engineering Solutions of Sandia, LLC, a wholly owned subsidiary of Honeywell International Inc., for the U.S. Department of Energy's National Nuclear Security Administration under contract DE-NA0003525.

TBD SAND #

Sandia National Laboratories

U.S. DEPARTMENT OF ENERGY NNSA

Sandia National Laboratories is a multimission laboratory managed and operated by National Technology & Engineering Solutions of Sandia, LLC, a wholly owned subsidiary of Honeywell International Inc., for the U.S. Department of Energy's National Nuclear Security Administration under contract DE-NA0003525.

Background & Motivation

Ab-initio methods

- High accuracy
- Spatial and temporal restrictions

Molecular dynamics (MD)

- Classical – lower accuracy
- ML-IAPs can improve accuracy
  - SNAP, GAP, ACE, etc.
- ML-IAPs often limited to small temperature/pressure range
- Challenges can arise …
  - Magnetism, phase changes, electron excitations, etc.

Ability to build transferable MD-IAPs highly desirable

- Enables examination of complex material/engineering problems

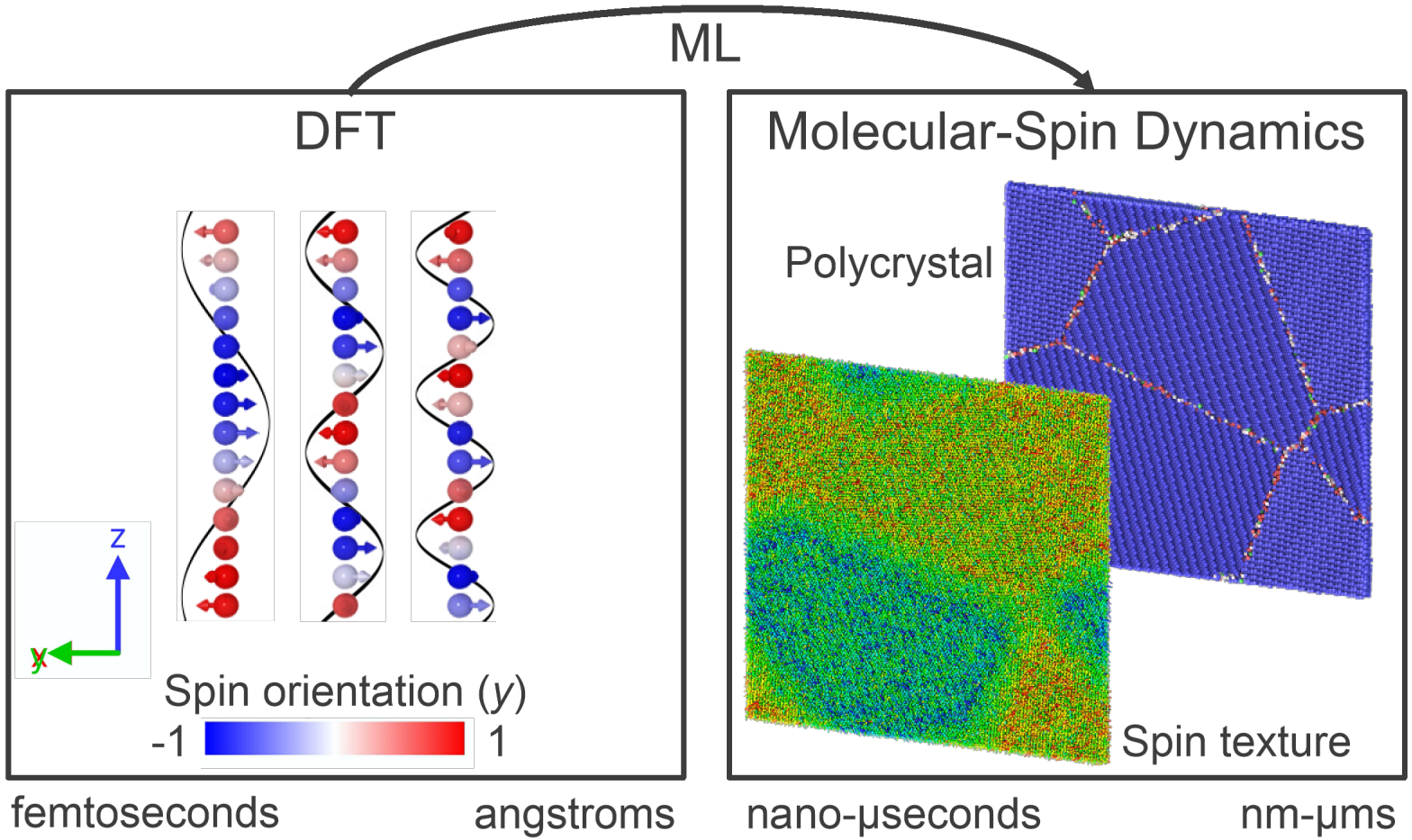

ML Framework for α-Fe

1) Generate ab-initio dataset for Fe (VASP)
   - Fe data generated for 0 - 7000K and 0 - 400 Gpa
   - Spin spiral data generated for different degrees of compression
2) Use genetic algorithm (GA) to parameterize spin Hamiltonian using spin spiral data
3) Subtract magnetic energies/forces/stress from DFT Fe data and train interatomic potential, $U(R)$, using GA
   - $U(R)$ built using spectral neighbor analysis potential (SNAP)
   - $E^i_{SNAP} = \beta_0 + \boldsymbol{\beta} \cdot \boldsymbol{B}^i$ and $F_j^{SNAP} = -\boldsymbol{\beta} \cdot \sum_{i=1}^{N} \frac{\partial \boldsymbol{B}_i}{\partial \boldsymbol{r}_j}$
4) Evaluate candidate on predetermined set of objective functions (OFs)
   - Using candidate SNAP potential and parameterized spin Hamiltonian
5) Continue GA until desired OFs accuracy is reached

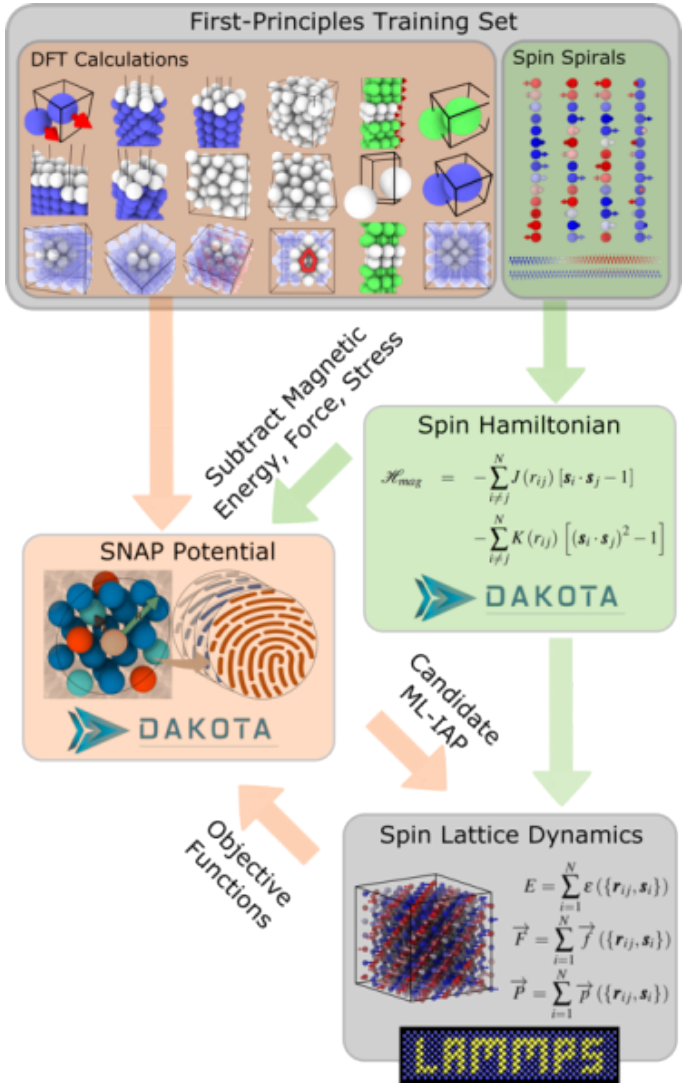

Magneto-Static Results for α-Fe

- Spin-spiral energy comparison between ab-initio calculations (VASP) and SNAP-Spin model
  - $\boldsymbol{s}_j = \sin(\theta)\cos(\boldsymbol{q}\cdot\boldsymbol{R}_{0j})\,\boldsymbol{x} + \sin(\theta)\sin(\boldsymbol{q}\cdot\boldsymbol{R}_{0j})\,\boldsymbol{y} + \cos(\theta)\boldsymbol{z}$
  - Compression along Γ point and also ΓH and ΓP high symmetry lines
  - DFT calculations ran using frozen magnon approach
    - 10x10x10 k-point grid used
    - 320 eV energy cutoff with 224 bands
- Good agreement between Molecular-Spin model and ab-initio calculations

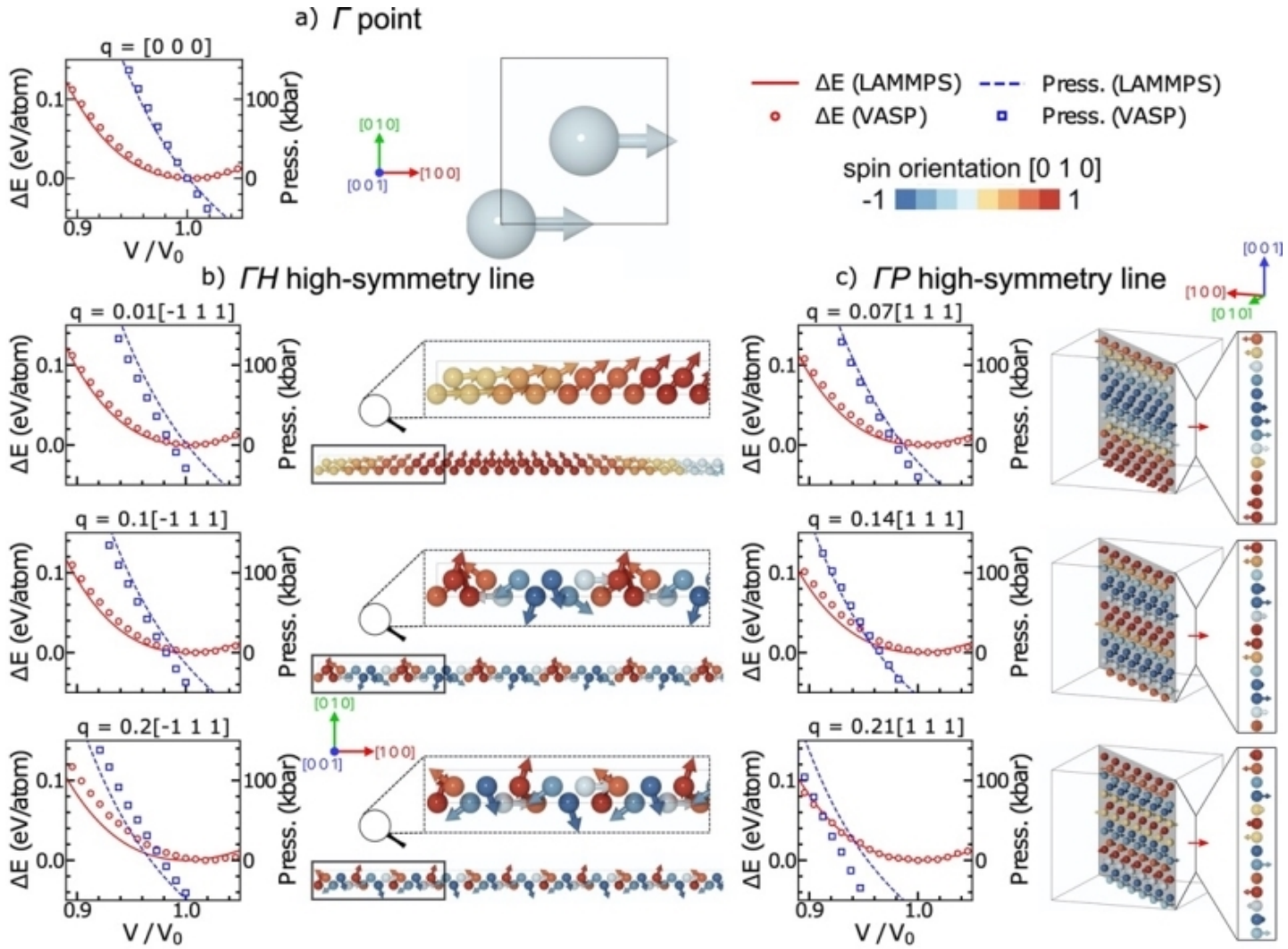

Example Results α-Fe (Fixed Magnetic Moment)

- Thermal conductivities (κ) calculated up to Curie temperature
- From Fulkerson *et al.*
  - $\kappa_T = \kappa_l + \kappa_e$
  - $\kappa_l = \kappa_p + \kappa_m$
  - Using κ_T, exp from Fulkerson $\kappa_{MSD,e}$ can be inferred as: $\kappa_{MSD,e} = \kappa_{T,exp} - \kappa_{MSD,p} - \kappa_{MSD,m}$
- Inferred electronic conductivity in good agreement with DFT
- Shear moduli & magnetostrictive coefficient high temperature behavior reproduced

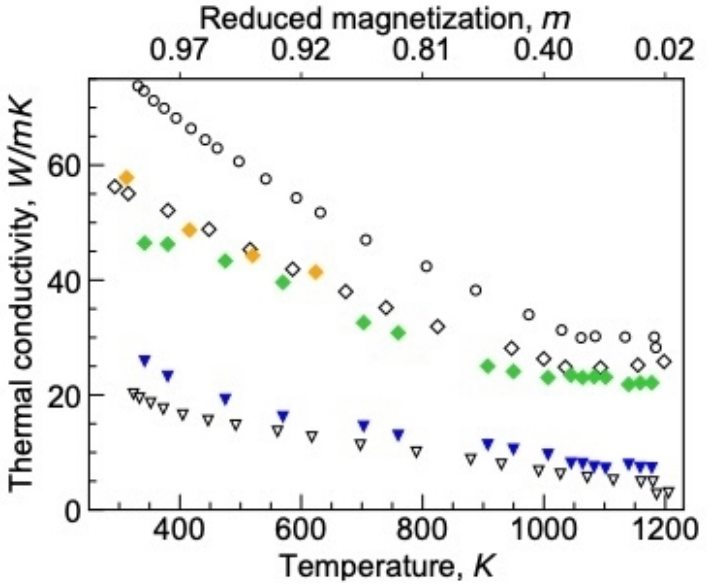

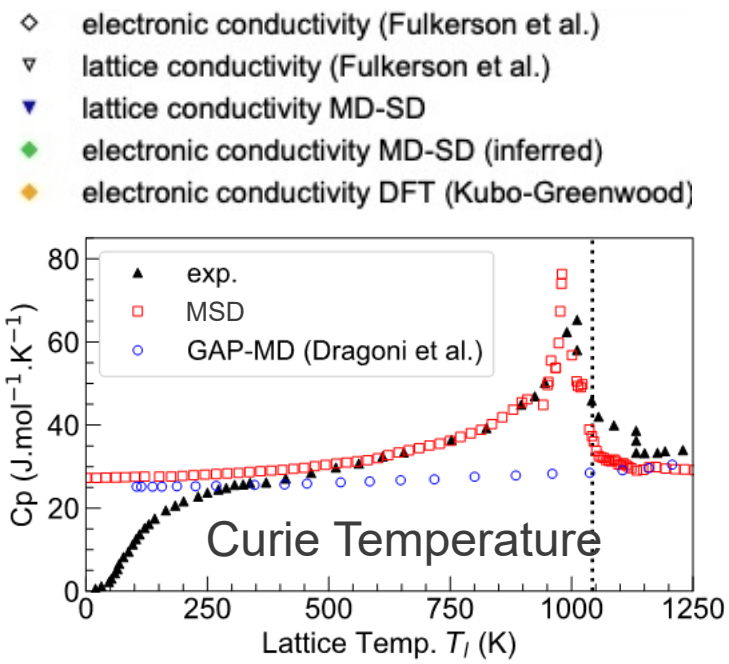

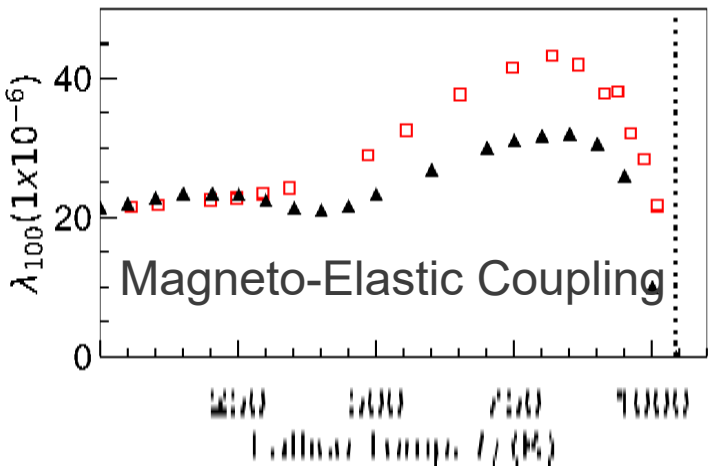

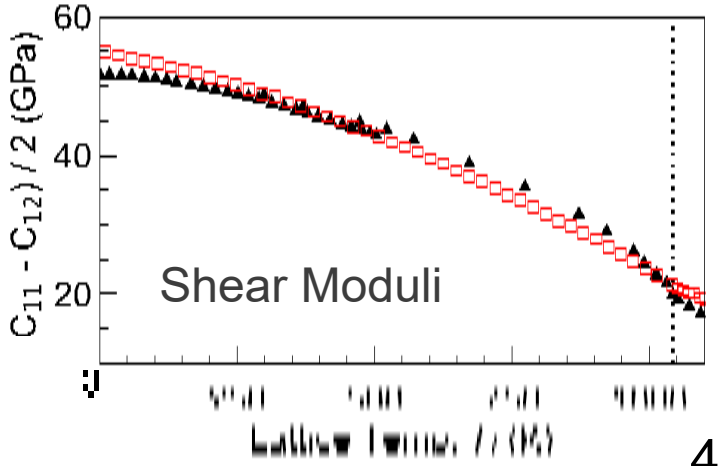

MSD Shock Model: Longitudinal Spin Fluctuations

- Longitudinal changes in magnetic vector
  - $\mathcal{H}_{Landau} = \sum_i (AS_i^2 + BS_i^4 + CS_i^6)$
  - $\hat{S}$ → spin vector of atom
  - $\hat{S} = \frac{-\hat{M}}{g\mu_B} = S_x\hat{\imath} + S_y\hat{\jmath} + S_z\hat{k}$
  - $S_i = \|\hat{S}\| = \sqrt{(S_x)^2 + (S_y)^2 + (S_z)^2}$
  - $A(p), B(p)$, and $C(p)$ are fitted to noncollinear spin data for iron†

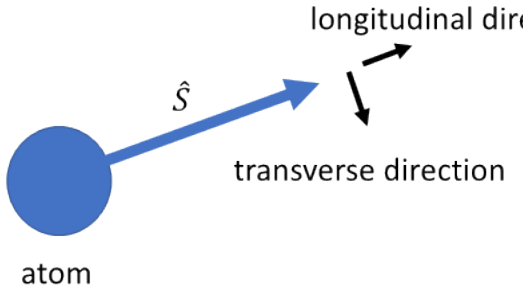

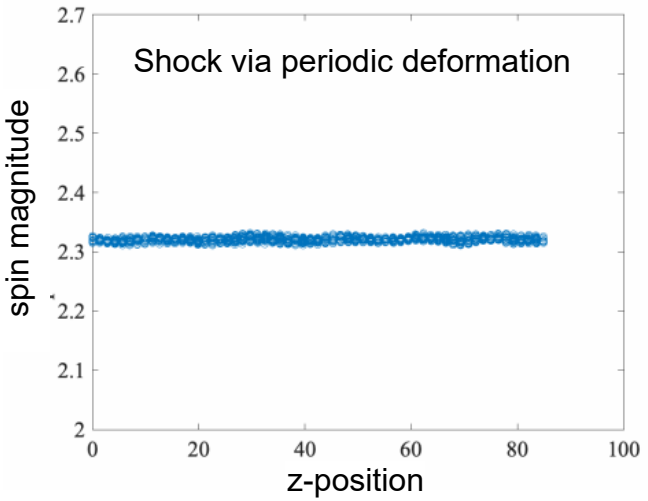

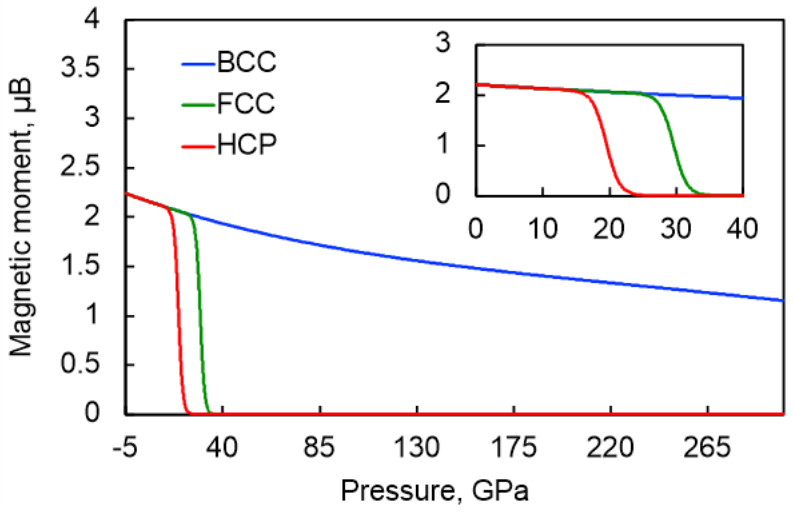

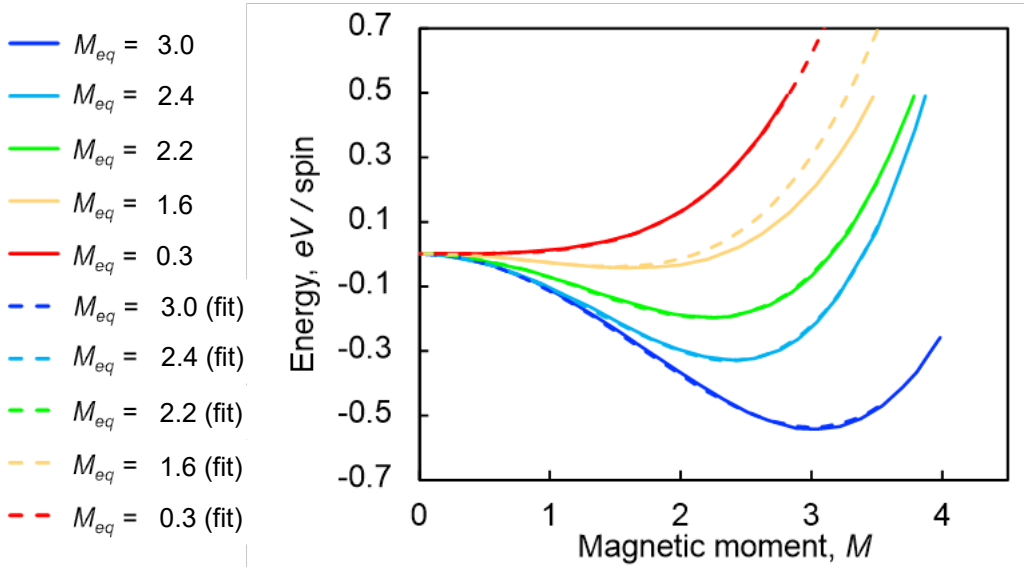

- Magnetic moment adjusted on the fly
  - Based on local pressure & phase

†Gambino, Davide, et al. "Longitudinal spin fluctuations in bcc and liquid Fe at high temperature and pressure calculated with a supercell approach." *Physical Review B* 102.1 (2020): 014402.

Alpha-Epsilon Transition: Longitudinal Spin Fluctuations

- Deforming box quasistatically in x-direction
- Increases in pressure lower BCC magnetic moments
- Once bcc-hcp transition starts magnetic moment distribution splits
  - Inducing associated changes in pressure
- Once material is fully in hcp regime (at higher pressures) magnetic moments are driven to zero

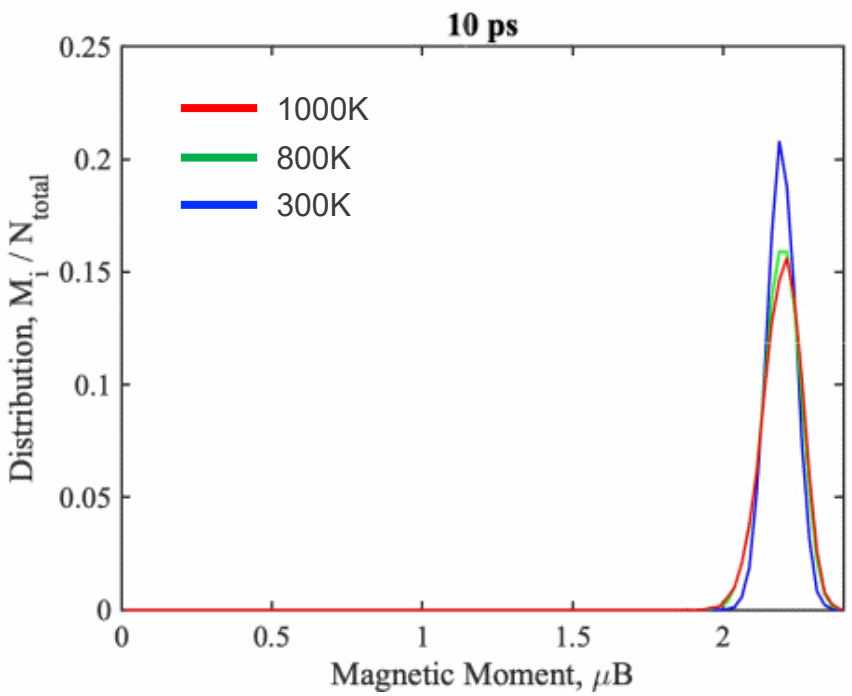

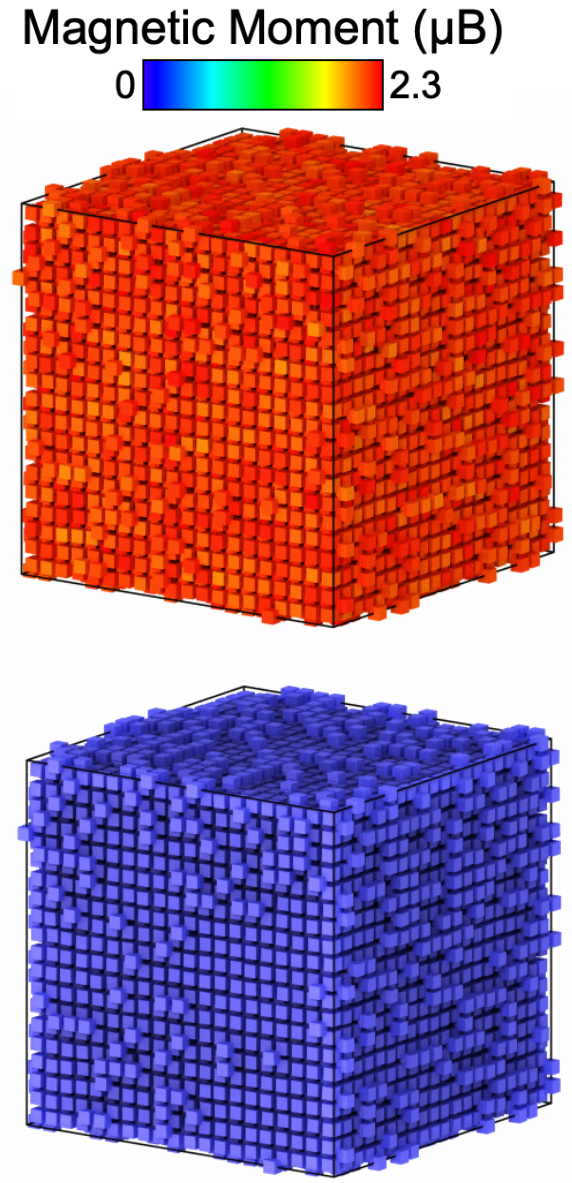

Alpha-Epsilon Transition: Longitudinal Spin Fluctuations

- Examined magnon/phonon spectra throughout the alpha-epsilon transition
- As transition to hcp state progresses acoustic/optical peaks shift to the right
- For magnon spectra the signal becomes significantly deteriorated as BCC frac. decreases
  - Due to weakening exchange interactions

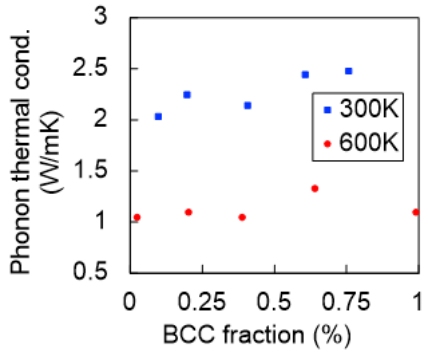

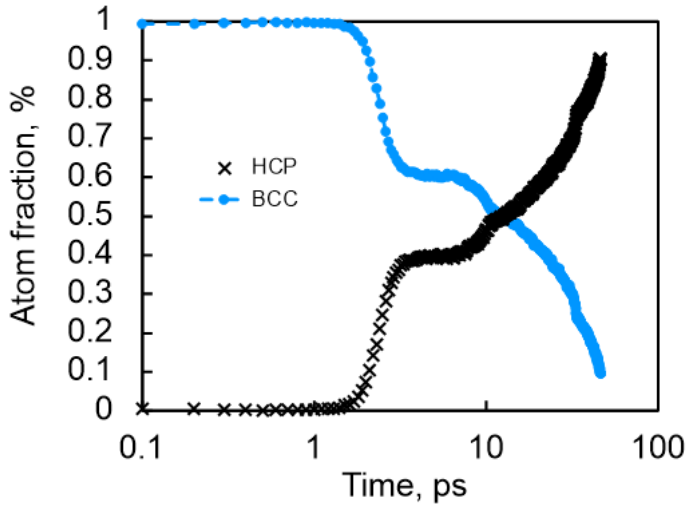

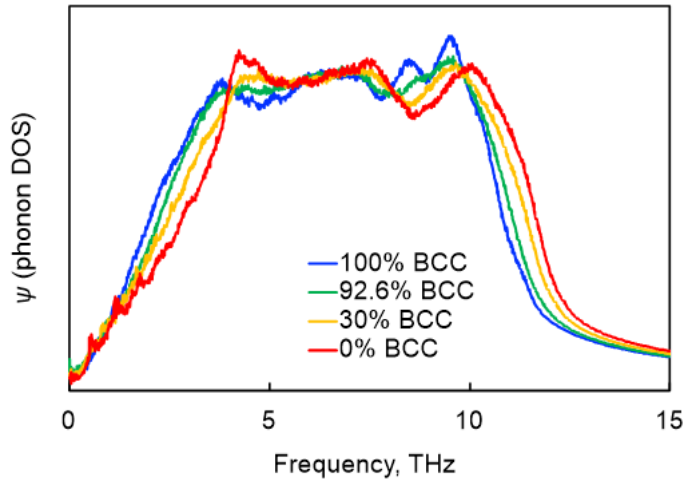

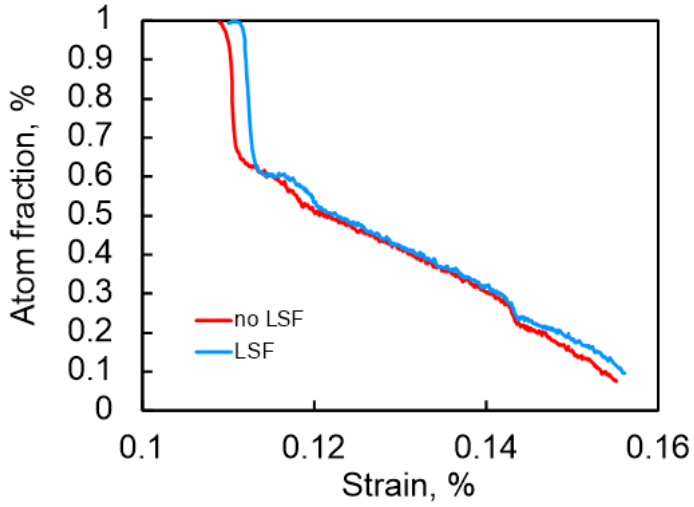

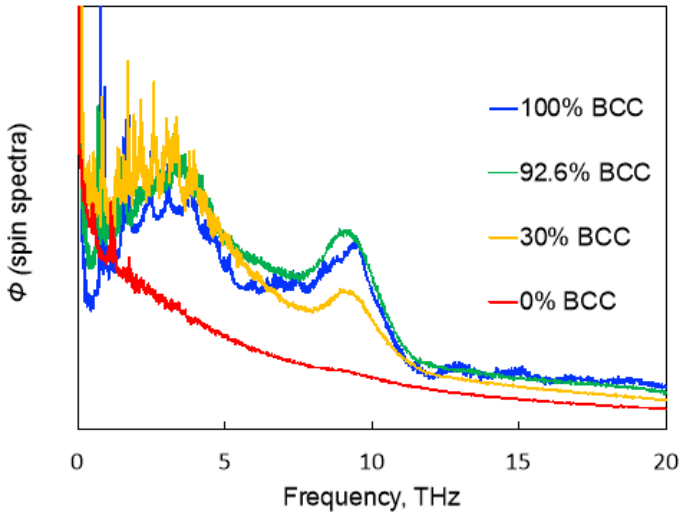

MSD Shock: Magnetic Response

- Examining angular velocity profiles
  - In fixed magnetic moment case shock drastically increases ω_z (Only pathway for high energy spin states)
  - LSFs weaken exchange interactions, decreasing ω_z (Some shock energy used to compress magnetic spin vectors)
- Measurable differences in pressure profile, ~5-30 Gpa
  - Observed in both elastic and plastic fronts

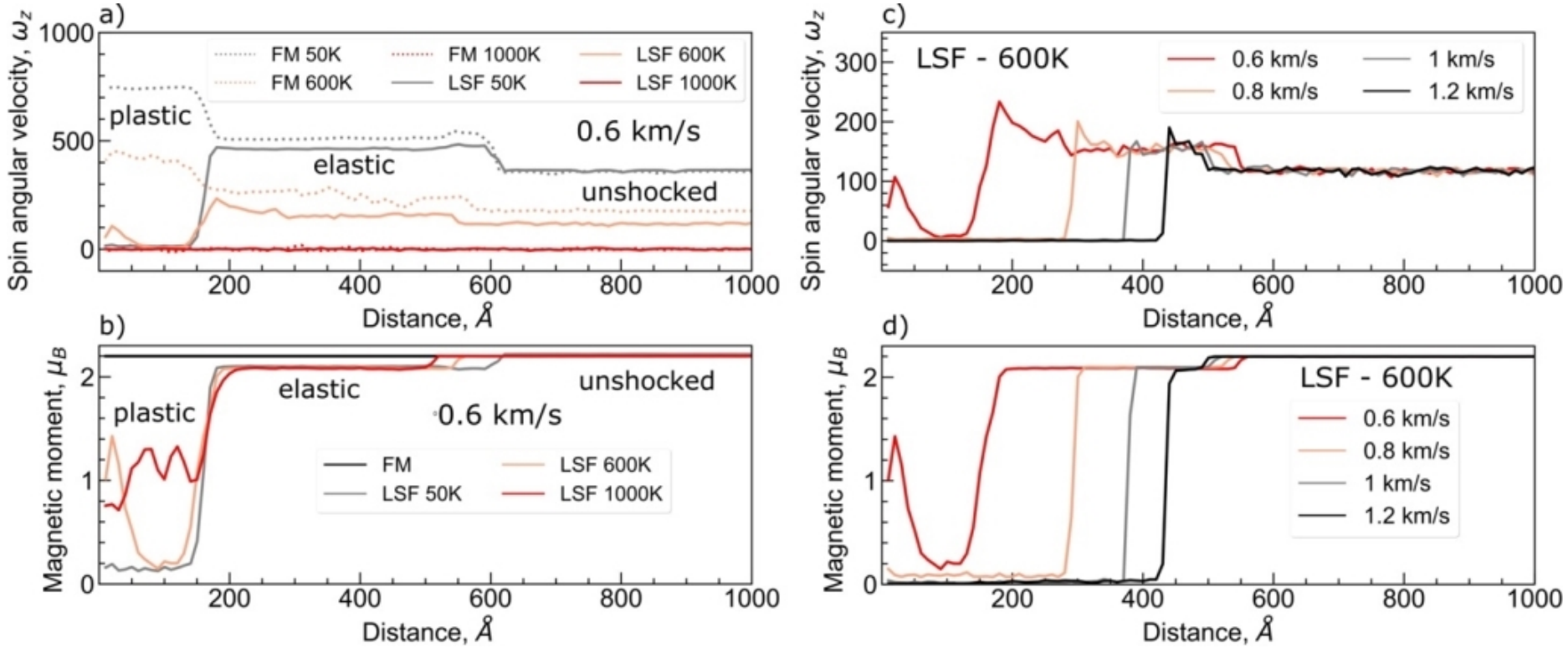

MSD Shock: Magnetic Response

- Tested multiple shock speeds near onset of α-ε transformation front
  - Lower magnetic moments observed near hcp / fcc phases
  - At lower shock speeds phase boundary tends to be more heterogeneous
  - Magnetic moments decrease in both elastic and plastic / transformation fronts

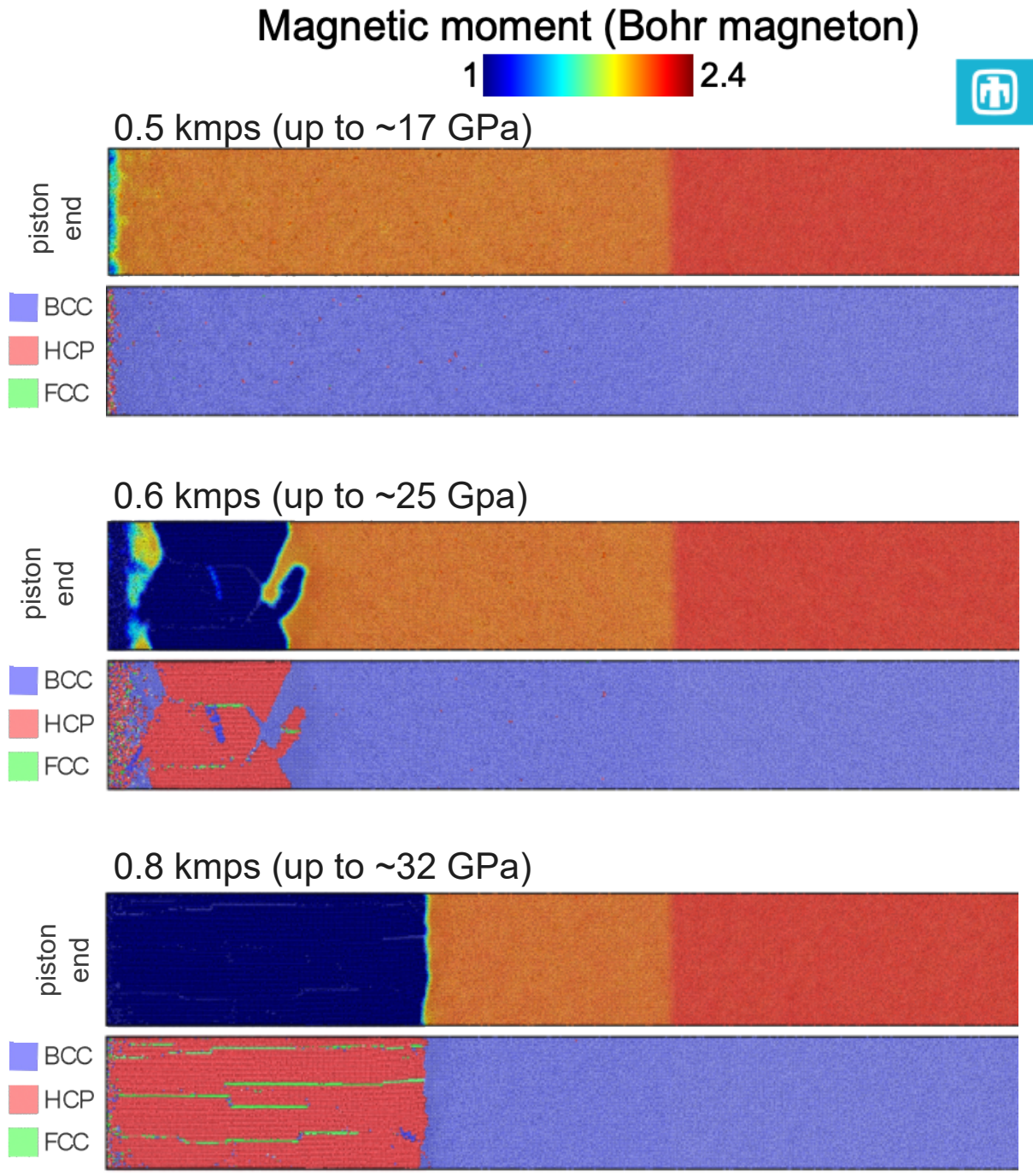

MSD Shock: Phase Diagrar

- Can recreate a shock phase diagram
  - Bin regions behind shock front and measure local T/Ps along with phase fraction
  - Allows us to probe Earth-core T/Ps
  - LSF model allows us to capture more accurate melt boundary

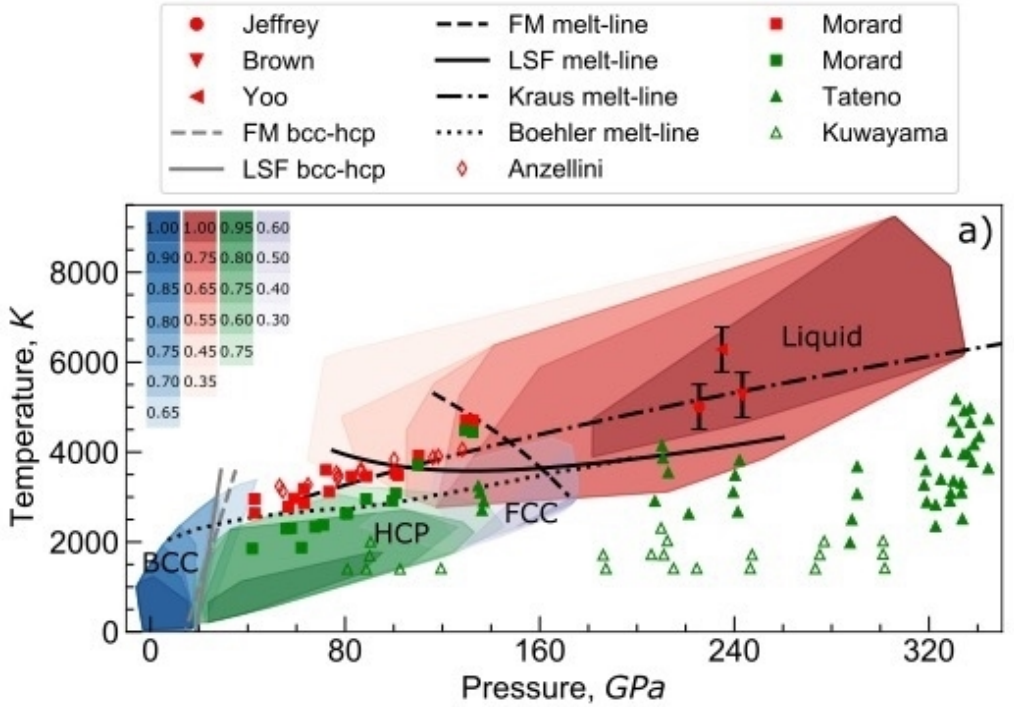

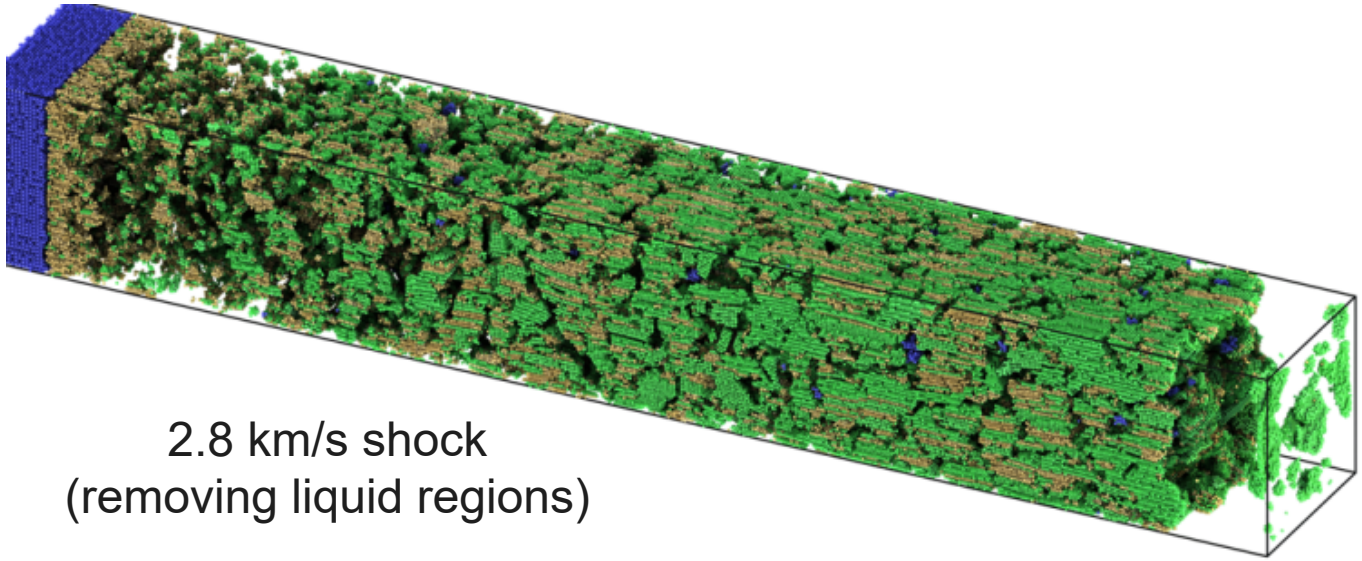

2.8 km/s shock
(removing liquid regions)

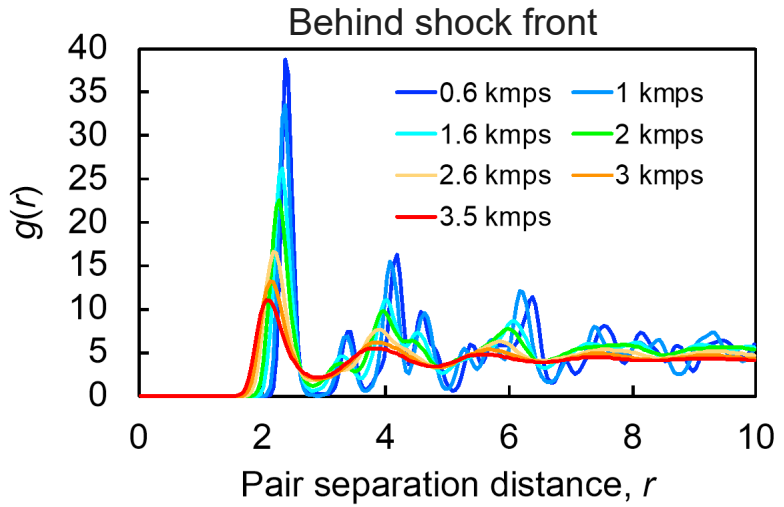

MSD Shock: Earth-Core Properties

- Examined P-wave velocities in 9.5-13.5 g/cc range
  - Near liquid-solid transition 2M & 16K cell results vary
  - Good agreement with PREM and liquid DFT data
- Adiabatic bulk modulus
  - Results within approx. 5-10% of EOS/PREM data
    - IAP results slightly stiffer
- Metastable bcc phase observed during melting

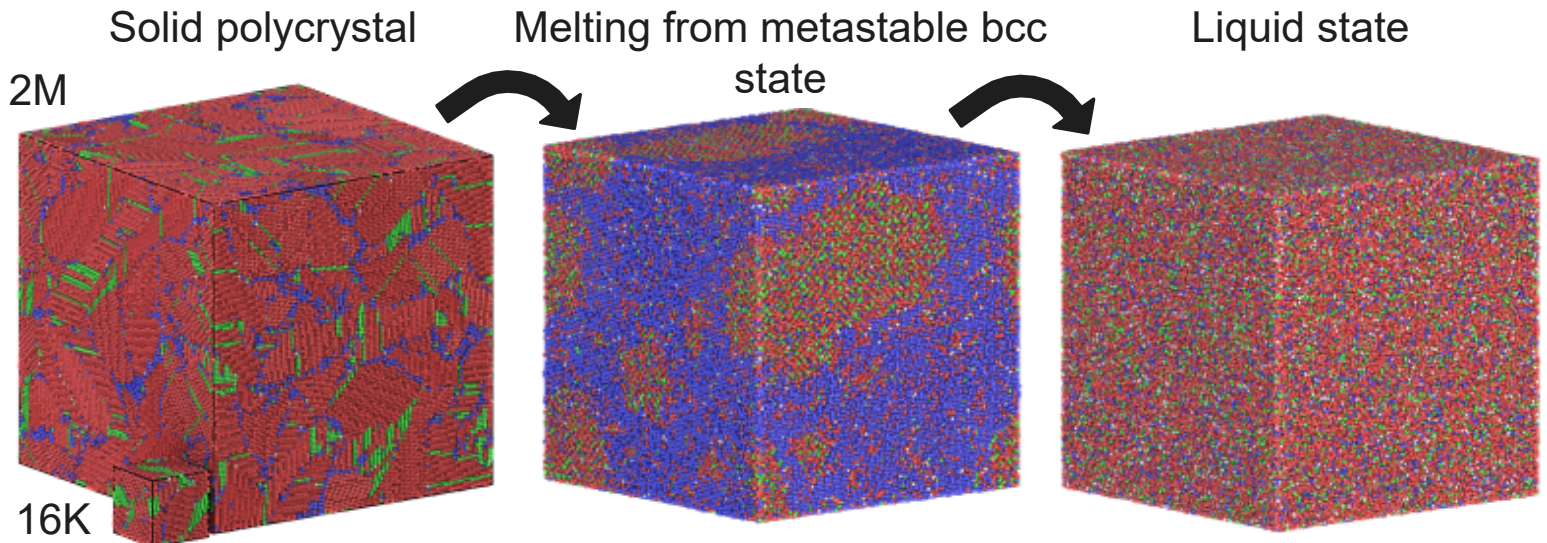

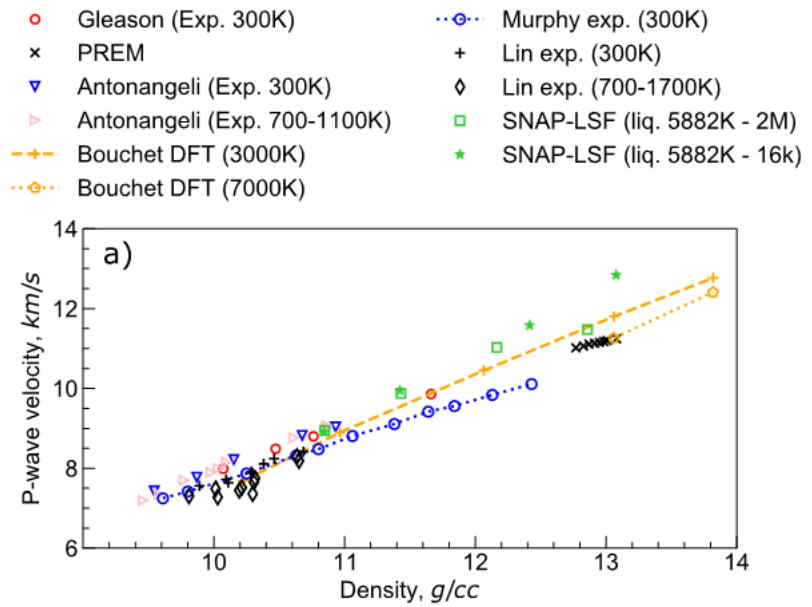

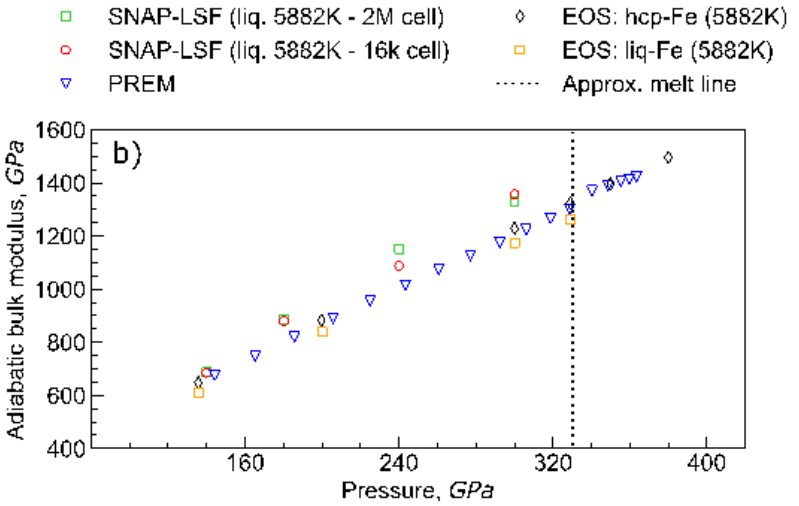

Copper Model Development: IAP Trained Using EOS Model Data

- Built new multi-phase EOS model for copper
  - Including electrical conductivity model
  - Based on existing experimental data and PBEsol DFT calculations
  - Resulting EOS tables tabulated in uTri format
  - Quantifying table uncertainty
  - Good agreement with exp. / DFT

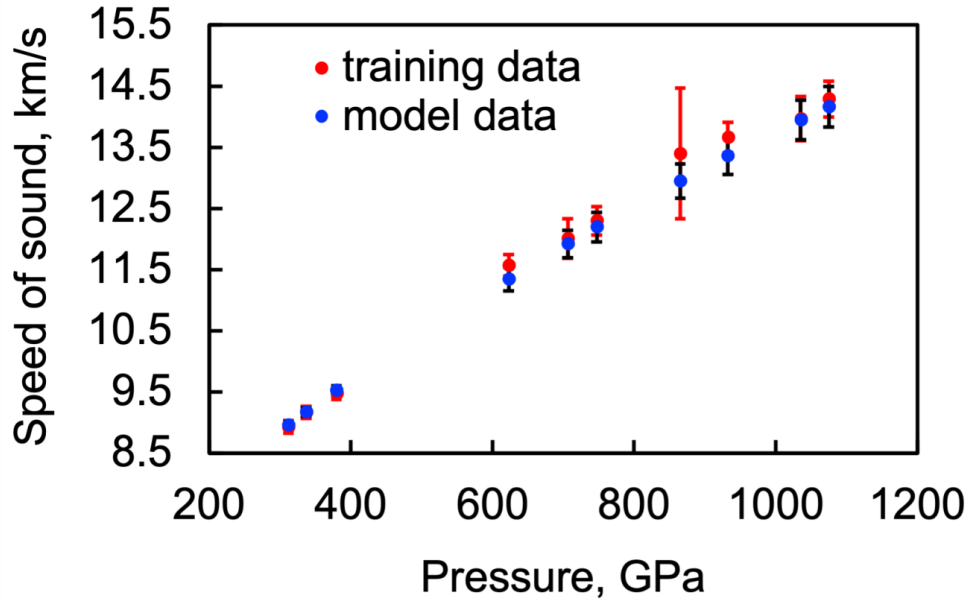

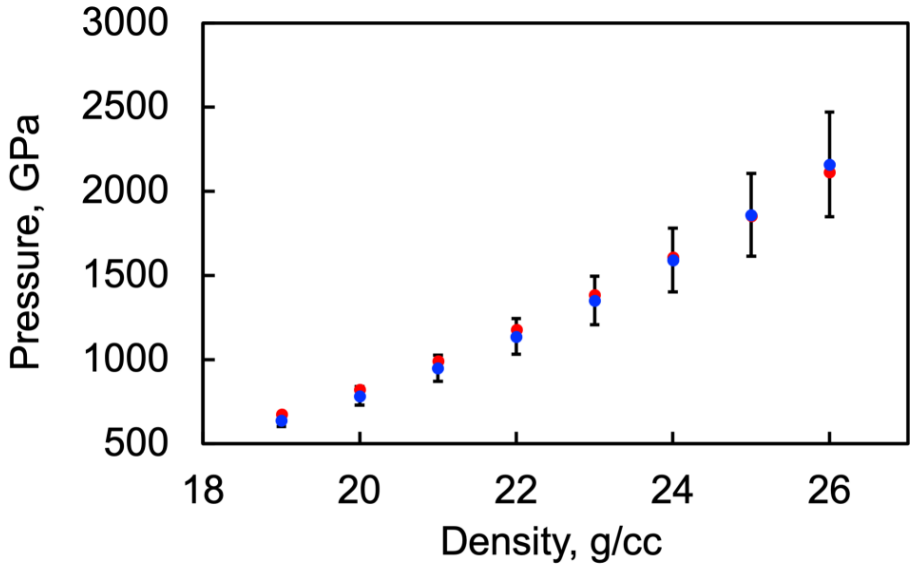

Copper EOS Model: Vapor

- DFT calculations carried out for low-density gaseous states
  - 7000 - 30,000 Kelvin
  - 0.1 – 6 g / cc
- Examined energy / pressure difference between DFT & EOS model
  - Good agreement with DFT calculations

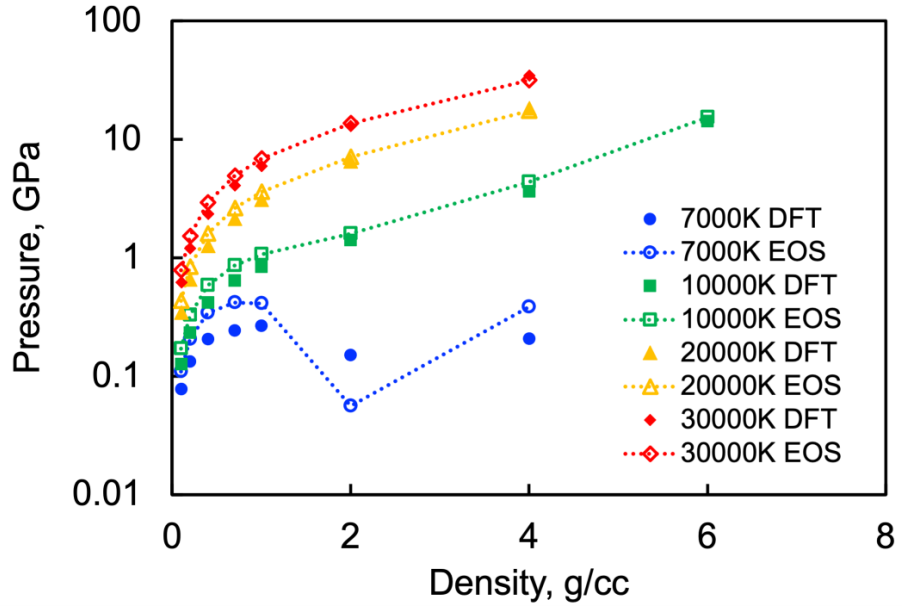

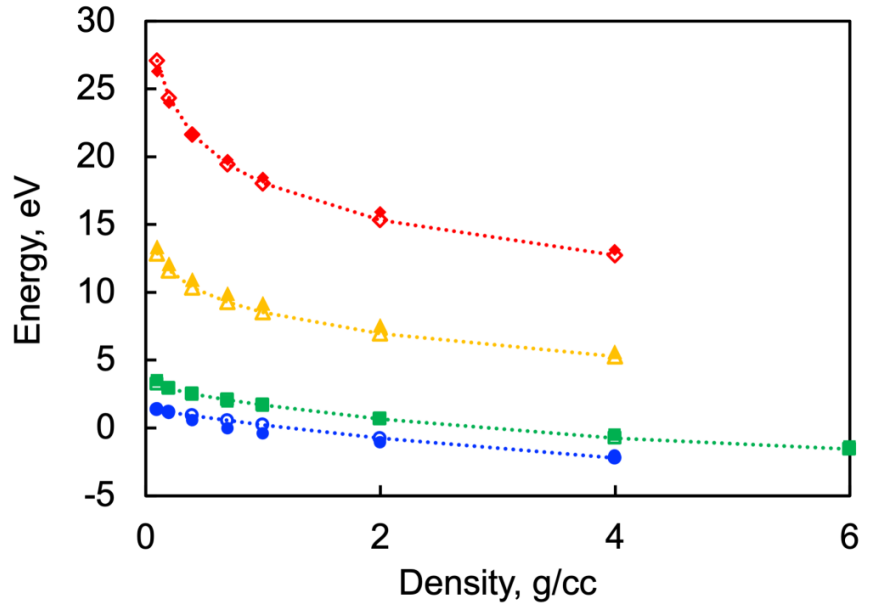

Copper EOS Model: Electrical Conductivity

- TD-DFT calculations used to measure electrical conductivities
- Electrical conductivity isobars based on exp. data
- Good agreement for both exp. / DFT data

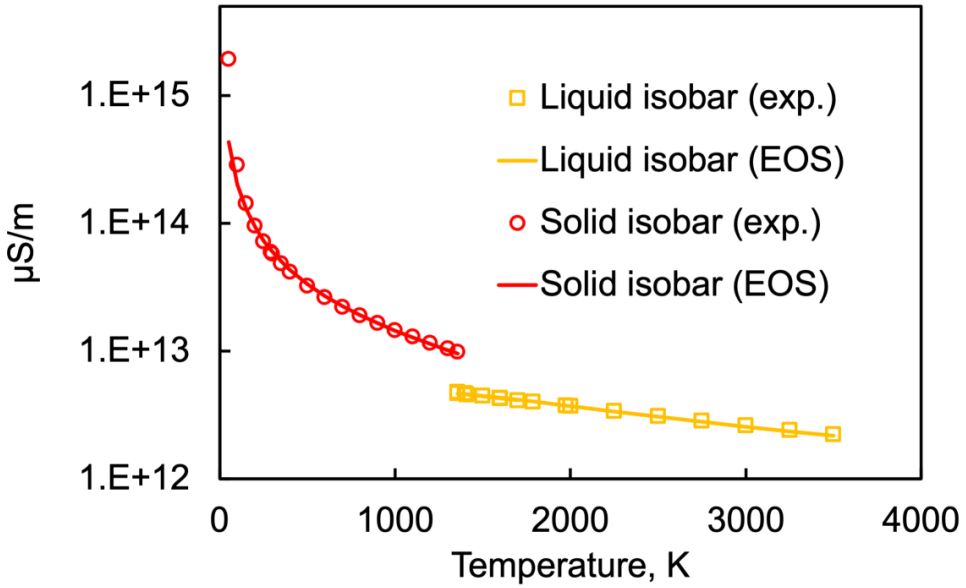

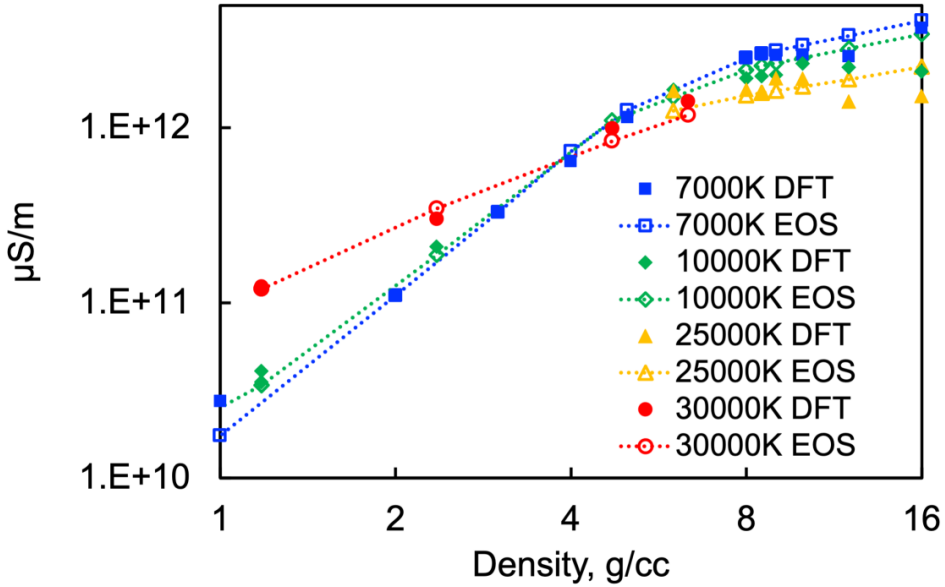

Copper Interatomic Potential Fitting

- Training SNAP interatomic potential(IAP) using nonlinear GA optimization
- DFT dataset range:
  - Density from 0.1-27 g/cc
  - Temperatures from 300-30,000K
- Goal: Develop a transferable interatomic potential for copper
  - Transferable → solid-liquid-vapor
- Main challenge:
  - Large changes in local environment
  - SNAP does not do well at very low densities

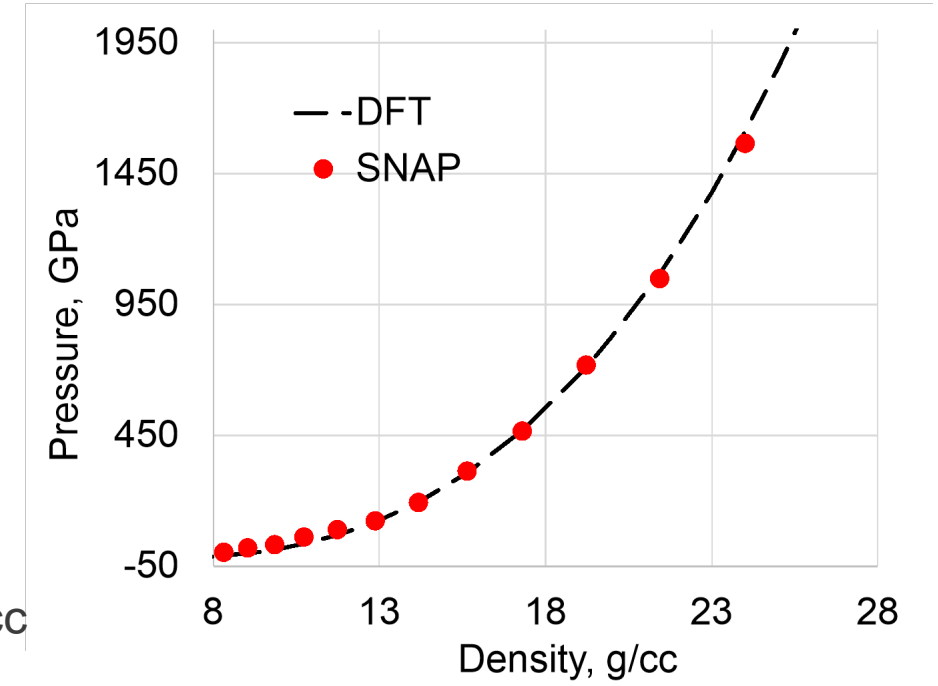

8000K & 0.8 g/cc

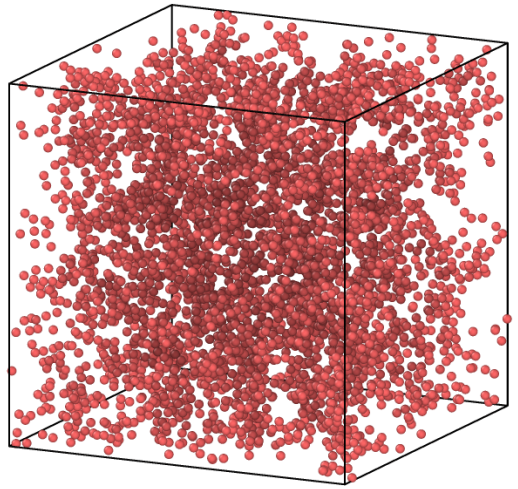

	0K elastic properties	
	Literature	SNAP
Poisson R.	0.42	0.42
BM	142	146.57
C11	176	179.95
C12	125	129.89
C44	81.7	72.77

Copper Interatomic Potential Fitting

Carried out quadratic SNAP fitting procedure with single objective function genetic algorithm

- Using reference potentials:
  - ZBL (short-range repulsion)
  - Morse (long-range interactions)
- Used ~20 groups with a population size of 1,000
- Ran genetic algorithm to approx. 40,000 candidates

Obtained interatomic potential that was stable in solid-liquid-vapor phases

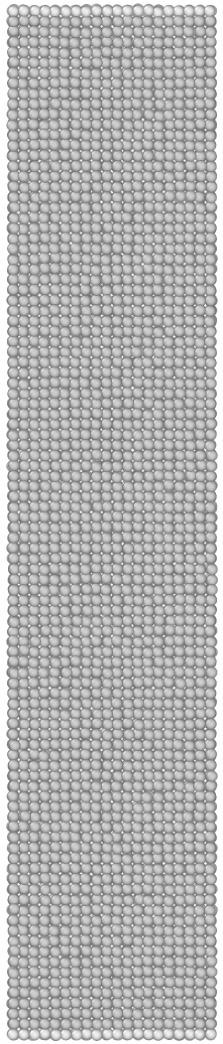

~2.5 kmps shock

Copper Interatomic Potential Fitting

Main outcome:

- Good transferability and phase stability achieved

Noteworthy issue:

- Difficult to capture vapor dome properties & high compression behavior with high degree of fidelity

Conclusion

- Extra flexibility needed in the long-range model

Analysis & next steps:

- Using best Cu SNAP potential the impact of Morse parameters were examined using Sobol sensitivity analysis

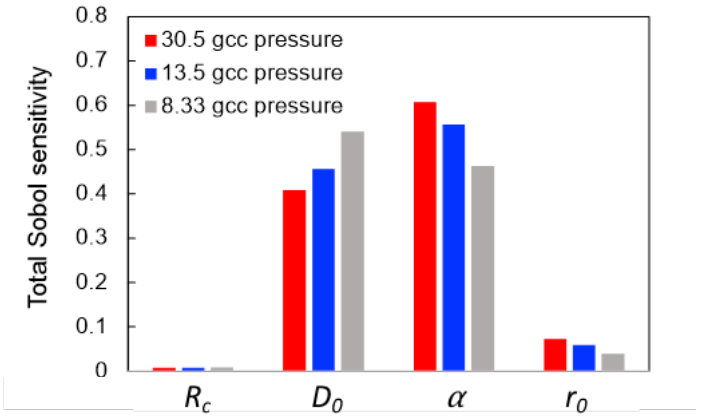

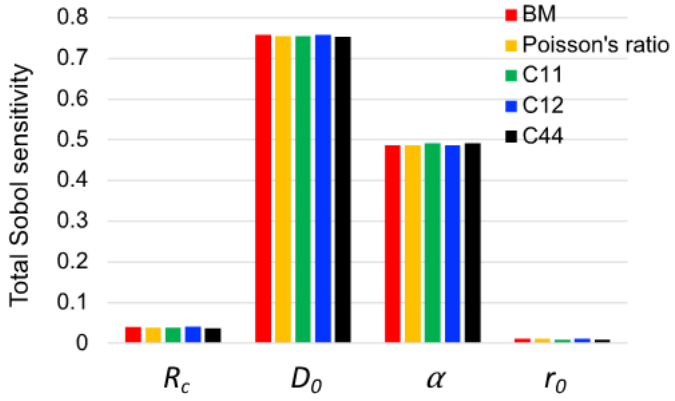

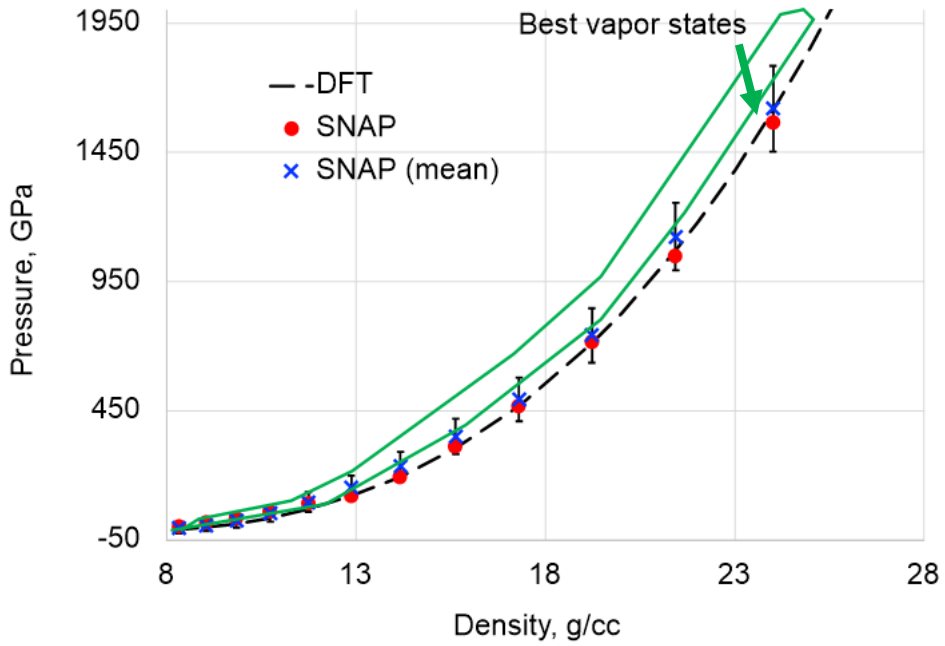

Copper Interatomic Potential Fitting

- Added a modified Morse pair style to LAMMPS
  - Changes added to morse/smooth/linear
  - $\phi(r) = D_0\left[e^{-2\alpha(r-r_0)} - 2e^{-\alpha(r-r_0)}\right]$
  - $E(r) = \phi(r) - \psi(r) - \phi(R_c) - (r - R_c)\frac{d\phi}{dr}\Big|_{r=R_c}$
  - $\psi(r)$ - switching function
  - $\psi(r) = \frac{1}{1+e^{br-d}}\phi(r)$
    - Where *b* controls the width of the transition and *d* controls the location of the attenuation (for a fixed *b*)
- This new pair style gives more flexibility to Bayesian optimization procedure
  - Important for building transferable interatomic potentials

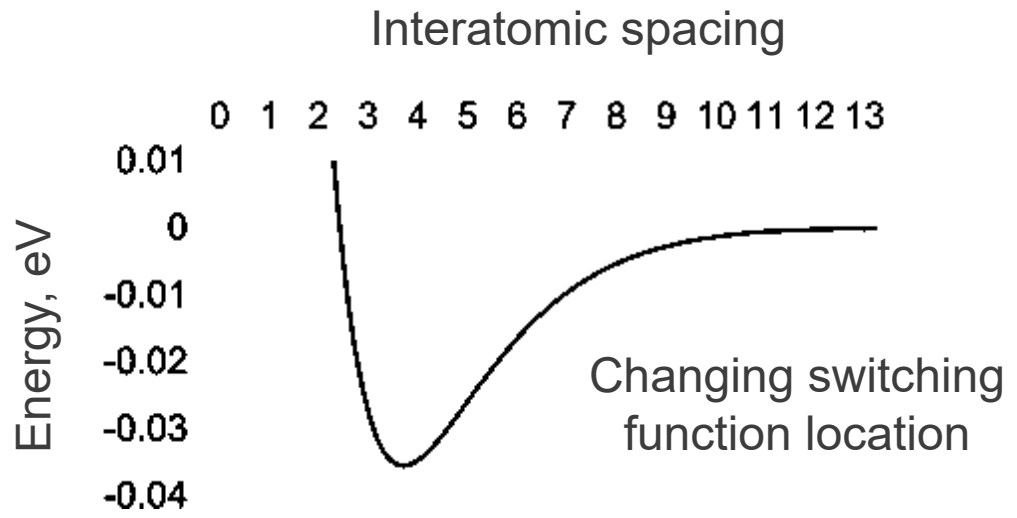

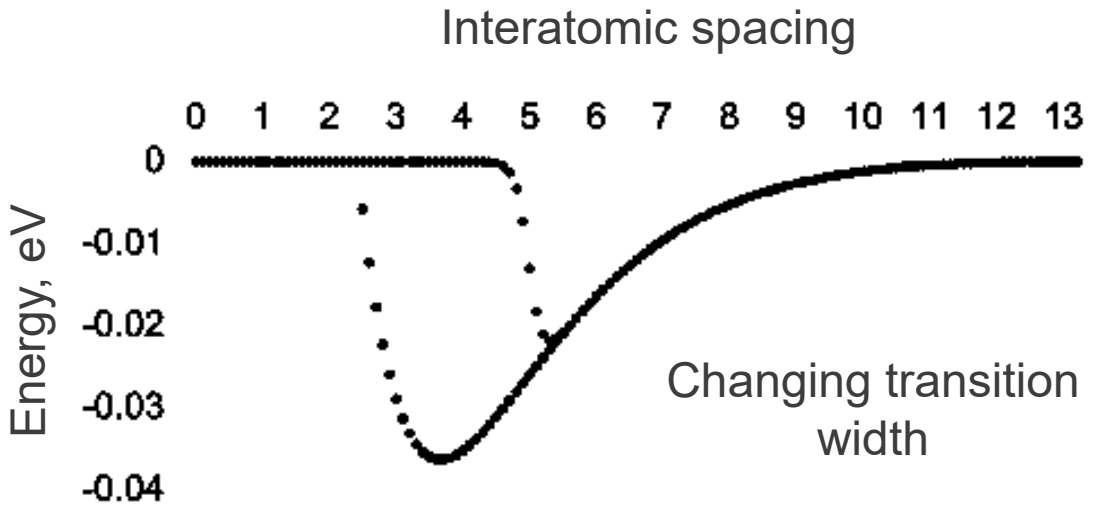

Copper Interatomic Potential Fitting

Nonlinear Dakota GA optimization

- Using adjusted Morse potential
- Using additional objective functions
  - 0K elastic properties
  - Cold curve
  - DAC data
  - Hugoniot points (both in solid/liquid regimes)
  - Cohesive energy
    - Check: FCC more stable than BCC
    - FCC/BCC energy difference ~ 0.02-0.1 eV/atom

Tested cold-curve agreement up to approx. 2TPa

- Good agreement with exp. data

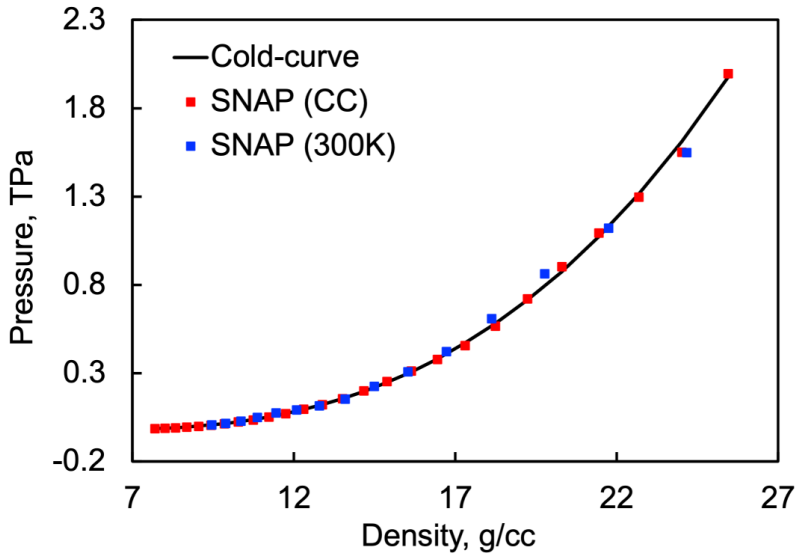

Copper Interatomic Potential Fitting

- Reasonable shock stability observed up to 8.6 km/s with latest potentials
  - Validation done using multi-scale shock technique (MSST) in LAMMPS
- Current efforts
  - Expanding shock stability to higher pressures
    - Up to 3 TPa
  - Gauging vapor stability for shock-stable potentials
    - Vapor dome calculations too costly for objective functions
      - Vapor calculations done in post-processing for best shock IAP potentials
        - Varying long-range Morse parameters

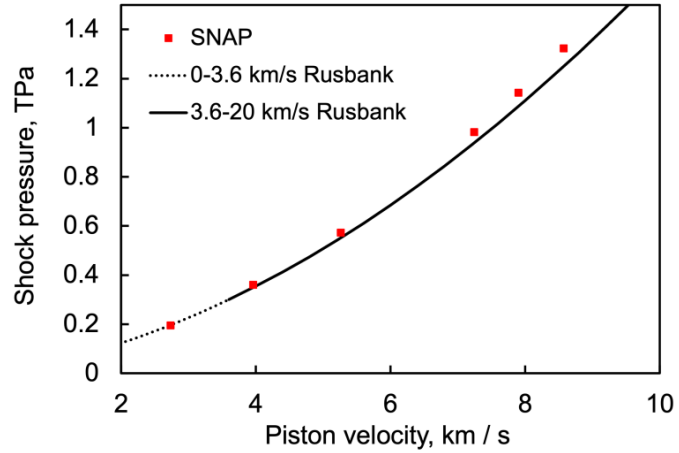

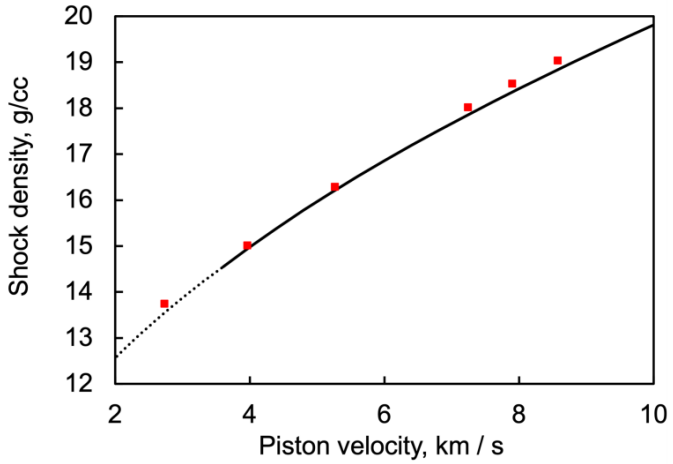

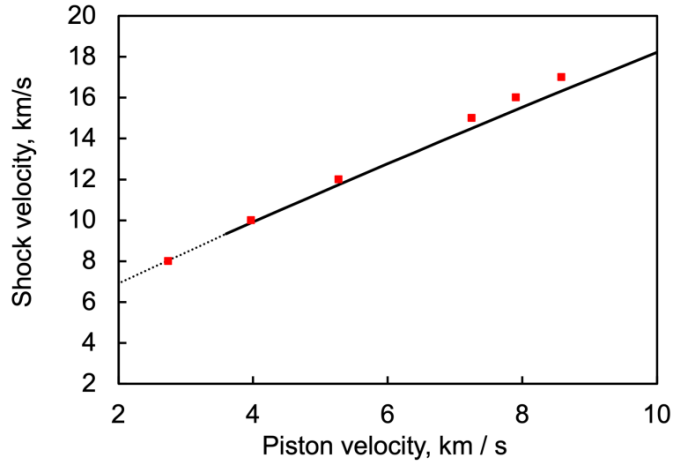

Conclusion

- Illustrated framework for building transferable IAP from ab-initio / exp. / EOS data
  - Complications from magnetics / long-range interactions
  - Incorporated longitudinal spin fluctuations
- Examined shock response of both Cu & Fe
- Fe shock stability up to Earth-core conditions
- Cu shock stability up to ~1.2 TPa

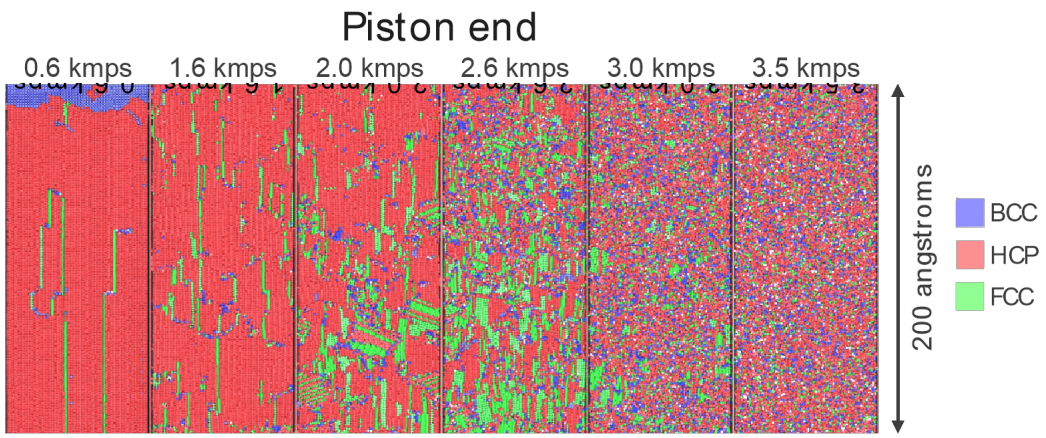

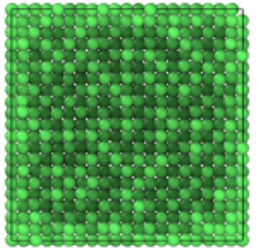

7.3 km/s MSST shock

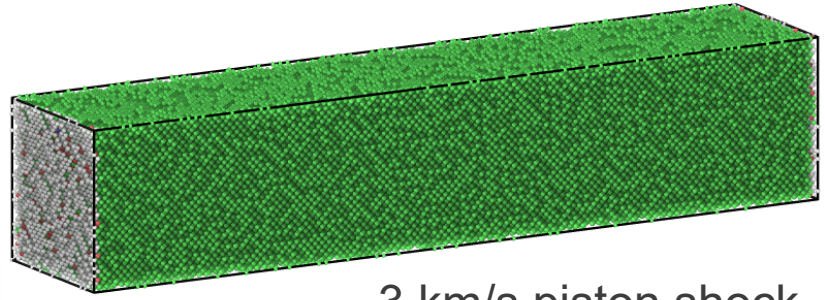

3 km/s piston shock

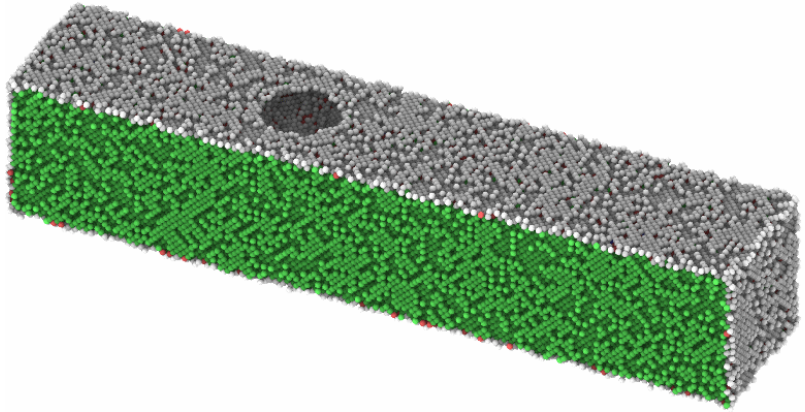

Piston hitting Cu nano-slab